Predicting re-emergence times of dengue epidemics at low reproductive numbers: DENV1 in Rio de Janeiro, 1986-1990.

Rahul Subramanian, Victoria Romeo-Aznar, Edward Ionides, Claudia T. Codeço, and Mercedes Pascual

Abstract:

Predicting arbovirus re-emergence remains challenging in regions with limited off-season transmission and intermittent epidemics. Current mathematical models treat the depletion and replenishment of susceptible (non-immune) hosts as the principal drivers of re-emergence, based on established understanding of highly transmissible childhood diseases with frequent epidemics. We extend an analytical approach to determine the number of 'skip' years preceding re-emergence for diseases with continuous seasonal transmission, population growth and under-reporting. Re-emergence times are shown to be highly sensitive to small changes in low R_0 (secondary cases produced from a primary infection in a fully susceptible population). We then fit a stochastic SIR (Susceptible-Infected-Recovered) model to observed case data for the emergence of dengue serotype DENV1 in Rio de Janeiro. This aggregated city-level model substantially over-estimates observed re-emergence times either in terms of skips or outbreak probability under forward simulation. The inability of susceptible depletion and replenishment to explain re-emergence under 'well-mixed' conditions at a city-wide scale demonstrates a key limitation of SIR aggregated models including those applied to other arboviruses. The predictive uncertainty and high skip sensitivity to epidemiological parameters suggest a need to investigate the relevant spatial scales of susceptible depletion and the scaling of microscale transmission dynamics to formulate simpler models that apply at coarse resolutions.

Introduction:

Epidemics of arboviruses such as dengue (1), Zika (2, 3), and chikungunya (4) result in substantial global morbidity. Over the past decade, invasions of several arboviruses have triggered large outbreaks in the Western Hemisphere. In Brazil, these invasions include dengue serotype DENV4 in 2012 (5) as well as Zika (2, 6) and chikungunya (7) between 2014-2016. Predicting and understanding the re-emergence of arboviruses after these invasions has important consequences for epidemic preparedness, particularly in regions where climate factors limit mosquito transmission in the off-season. These regions typically exhibit highly intermittent seasonal epidemics, lasting one to three years with long periods of no, or low, reported cases in between, and low mean reproductive numbers (the number of secondary cases arising from each primary case in a completely susceptible population, R_0) (5, 8-10). Several proposed explanations include the depletion of susceptible individuals following initial epidemics (11) and the time required for their replenishment via population growth (12), inter-annual variation in climate (13-17), and antigenic interactions between strains of different serotypes (18-21). These temporal patterns contrast with the recurrent seasonal outbreaks observed in childhood diseases with high reproductive numbers, whose extensive study has provided the basis for our theoretical understanding of SIR (Susceptible-Infected-Recovered) dynamics in infections that confer lifelong or lasting immune protection (22-29).

Statistical models of dengue transmission that take into account climate dependencies can be used to make short-term re-emergence forecasts on the order of 4 months (30) or 16 weeks (15). Many epidemiological models that predict the re-emergence of arboviruses such as Zika (11, 31) on longer time-scales of a year (11) or

several decades (31) rely however on compartmental formulations such as SIR-type approaches (11) or Ross-McDonald equations that explicitly incorporate vector transmission (31). Both formulations assume transmission between any two individuals in the population ('well-mixed' conditions), typically at aggregated spatial scales. These process-based formulations, for example those recently applied to Zika, represent the acquisition of immunity in the population and its loss via demographic growth and turnover. These models do take into account seasonality of transmission and spatial heterogeneity in the intensity of transmission due to climate at coarse resolutions (at large city, state, or country-level scales). Nevertheless, the replenishment of a well-mixed susceptible population is the principal driver determining when the disease will re-emerge given a particular seasonal pattern for R_0 at a particular location. Stochasticity can also play an important role in long-term models of re-emergence (31). Variation in reporting rates of arboviruses between locations (32) can add further complexity.

Although childhood diseases with high reproductive numbers display different dynamics from emergent arboviruses (22-26), their compartmental models share a basic SIR structure given the acquisition of long-term immunity after infection. The resulting depletion and replenishment of the susceptible population is known to clearly drive inter-annual variability and re-emergence in the former (25, 27, 28). In particular, recent theory (29) has derived analytical expressions for the number of "skip" years for a measles-like disease in the pre-vaccine era, where "skips" are defined as seasons when transmission occurs but does not cause susceptible depletion. In other words, although the number of infections increases in such seasons, it is not large enough to offset the growth in the susceptible population due to demography. The resulting expressions specifically provide a threshold condition for the number of skips expected

following an initial invasion as a function of R_0. Their derivation did not include under-reporting and assumed a closed-population SIR model with 'school-term' seasonality, alternating two different rates for low and high transmission.

We examine in this work whether replenishment of susceptible individuals under the typical 'well-mixed' assumption explains dengue (DENV1) re-emergence at the whole-city aggregated level. We specifically address the uncertainty inherent in such predictions at the low reproductive numbers characteristic of arboviruses, not previously considered in applications of the analytical approach. To this end, we first extend the threshold derivation to take into account population growth, continuous (sinusoidal) seasonality, and under-reporting of cases. We then fit a stochastic SIR model to observed monthly dengue case counts from the DENV1 invasion in Rio de Janeiro, Brazil from 1986-1988 (8, 10, 33) and numerically predict expected times to re-emergence. We describe high uncertainty in re-emergence times for these seasonal, low transmission regions, and show the insufficiency of susceptible replenishment in a simple SIR model to explain the short periods observed in DENV1 re-emergence. We discuss possible explanations and the need for model formulations that would scale to coarse spatial resolutions.

Results:

We start with the analytical approach for a seasonally forced SIR system with intermittent outbreaks and population turnover, to consider general features of re-emergence at low R_0. In such a system, the onset of the off-season can bring an end to an initial outbreak, and the replenishment of susceptible individuals due to births and population turnover can be a major determinant of recurrence times. Let S represent the

number of susceptible individuals in a population and s_0, the fraction of the population still susceptible at the end of an initial epidemic, t_0, when a prediction for the time to the next outbreak will be made. If there are enough susceptible individuals left in the population (i.e. if s_0 is large), another outbreak will occur in the following year once the on-season resumes. However, if the initial outbreak was very large, s_0 may be too small, and the outbreak may "skip" one or more years. A skip year is defined as a year in which the susceptible population does not decrease, whether or not infections increase. The smaller the fraction of the susceptible population at the time of prediction (s_0), the longer it will take for the susceptible population to replenish, and the larger the number of skips that will occur. Previous theory allows prediction of the number of skips that will occur given s_0. Specifically, it demonstrated that s_0 must fall below some threshold s_c (k) for k skips to occur. An analytical expression was provided for s_c(k) in terms of the reproductive number and population turnover rate for a closed-population SIR model with school-term seasonality (29). The derivation of the threshold presented in (29) requires the assumption that the transmission rate or reproductive number of the disease is high and that the fraction of the population susceptible at the time of prediction (s_0) is small.

We extend this approach to take into account population growth and sinusoidal seasonality (which describes the transmission rate of dengue more accurately than a discrete high-low representation). Our derivation does not require assuming that the transmission rate or reproductive number are high or that the fraction of the population susceptible at the time of prediction is small. We follow the criteria developed in (29) (see details in (34)), which essentially consider the sign of the logarithm of the ratio between the respective number of infections at two times, t_0 and t_n>t_0. A positive value indicates that an outbreak will still occur at t_n; conversely a negative value indicates no outbreak at

that time. By setting the logarithm of this ratio to zero, the threshold s_c is obtained (See Section 1 of the Supporting Information for details).

The resulting expression for $s_c(n)$, the critical fraction of susceptible individuals required at the time of prediction for *n* or more skip seasons to occur, is

$$s_c(n) = 1 + \frac{\pi(2n+1)(1-\frac{1}{R_0})-2\delta}{\omega f(\omega,\delta,r,n)} \qquad (1)$$

where $f(\omega,\delta,r,n) = (1+e^{-r\frac{\pi}{\omega}(2n+1)})\omega\,\delta/(\omega^2+r^2) - (1-e^{-r\frac{\pi}{\omega}(2n+1)})/r$, R_0 is the annual mean of the reproductive number, δ, the amplitude of seasonal transmission (as infectious contacts per person per day), ω, the transmission frequency (in days^{-1}) and *r*, the population growth rate (also in days^{-1}). The full expression for the seasonal transmission rate is given by $\beta(t) = \beta_0(1+\delta sin(\omega t+\phi)$, where ϕ corresponds to the phase (in radians) and β_0, to the mean seasonal transmission rate (infectious contacts per person per day). The quantity β_0 is related to the annual mean reproductive number R_0 via the expression $R_0 = \beta_0/\gamma$, where γ is the recovery rate (in days^{-1}).

Figure 1 illustrates the implications of this formula. As before, t_0 corresponds to the time of prediction, in practice usually after a large initial epidemic or invasion. Likewise, s_0 represents the fraction of the population susceptible at the time of prediction. Intuitively, the smaller the fraction of the population susceptible at the time of prediction (s_0), the longer it will take for the susceptible population to replenish, and the larger the number of skips that will occur. In practice, as we will illustrate below, values of s_0 can be computed from surveillance data provided one has an estimate of the reporting rate.

For *n* skips to occur, the fraction of the population susceptible at the time of prediction (s_0) must fall below the susceptibility threshold $s_c(n)$. Figure 1A shows that the larger the number of skips *n* one is considering, the smaller the threshold $s_c(n)$ that s_0

must fall below for at least n skips to occur. Let n_c denote the critical skip number corresponding to the number of skips expected at the time of prediction (t_0). We use the fraction of the population susceptible at the time of prediction (s_0) and identify the maximum value of n for which s_0 is smaller than $s_c(n)$. In the example shown in Fig. 1A, this fraction $s_0 = 0.7$ is smaller than $s_c(n = 6)$ and bigger than $s_c(n = 7)$, which means $n_c = 6$. We therefore expect six years of skips followed by re-emergence in the seventh year. Formally, for a given value of s_0 at the end of the transmission season, we define the critical skip number n_c as the value of n for which $s_c(n_c) > s_0 > s_c(n_c + 1)$.

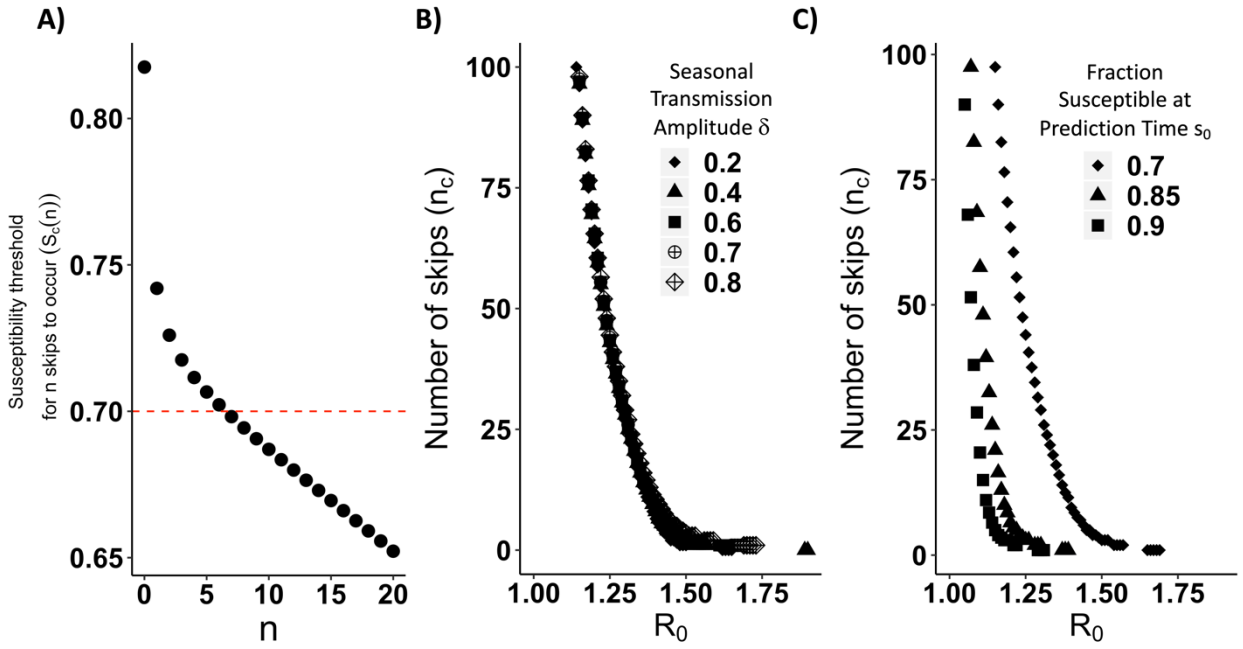

Fig 1. A) Graphical illustration of how the expected number of skips (n_c) is calculated. The black dots represent the threshold fraction of the population susceptible at the time of prediction required for n skips to occur ($s_c(n)$). The plot shows (s_c(n)) as a function of n (the number of skips) obtained from Equation 1 with seasonality amplitude δ=0.2 (contacts per person per day) and reproductive number R_0=1.4. In this example, the red line represents the fraction of the population susceptible at the time of prediction (s_0). If s_0 is smaller than s_c(n), at least n skips will occur. To find the expected number of skips (n_c), we identify the largest number of skips n such that s_0 is smaller than the susceptibility threshold required for those skips s_c(n). In this example, the red line intersects the $s_c(n)$ curve between $s_c(n$=6) and $s_c(n$=7). Therefore, a critical skip number

of n_c=6 is obtained. **B) and C) The critical skip value n_c as a function of R_0** for (B) different values of the amplitude of seasonal transmission δ with s_0=0.7 and (C) different values of the fraction of the population susceptible at the time of prediction (s_0) with δ=0.70. In all three panels, the frequency of transmission ω, the population turnover rate μ, and population growth rate r are fixed at respective values $\omega = (2\pi/365)$ day^{-1} corresponding to an annual periodicity, $\mu = 1/(74.46*365))$ day^{-1} corresponding to an average lifespan of ~75 years, and $r=1.55\mu$ day^{-1} consistent with the growth of the city of Rio de Janeiro. These values were chosen for the purpose of illustration, based on the inverse of the average life expectancy in Brazil in 2012 according to the 2010 census (35), and the interpolation of population estimates for the resident population of the municipality of Rio de Janeiro from the 1991 (36) and 2000 (37) censuses assuming exponential growth.

With this general approach at hand, we explored the effects of the reproductive number R_0, amplitude of seasonal transmission δ and fraction of the population susceptible at time of prediction s_0, on the critical number of skips n_c (Figure 1 Panels B and C). Consideration of both the variation of the reproductive number R_0 and fraction of the population susceptible at time of prediction s_0 is relevant here. Different combinations of transmission rate (β_0) and duration of the infection ($1/\gamma$) can yield the same R_0 but different fractions of the population susceptible at the time of prediction (Supplemental Figure S16). Importantly, Fig. 1 panels B and C show that the time to re-emergence is very sensitive to R_0. A singularity is observed as R_0 approaches 1 where the expected number of skips goes to infinity. The approach to that singularity can be very steep, meaning that small changes in R_0 can result in large increases in the expected re-emergence time. The obtained values of n_c are not as sensitive to the amplitude of seasonal transmission (Fig. 1 Panel B) but are sensitive to the fraction of the population susceptible at the time of prediction (Fig. 1 Panel C). The shift of the curve in Fig 1 Panel C for small values of the fraction of the population susceptible at time of prediction s_0 means that, for a given R_0, more time is required to replenish the susceptible population and therefore to observe a re-emergence.

We next apply this approach to the surveillance data from the 1986 invasion of DENV1 in Rio de Janeiro (Figure 2). The initial DENV1 invasion in Rio de Janeiro is an ideal initial test case for this technique given the lack of widespread prior immunity from to prior dengue epidemics, vaccination campaigns, cross-immunity from other disease outbreaks. Specifically, the 1986 invasion occurred prior to the development of dengue vaccines. The outbreak was the first dengue invasion in the area since the initial eradication of the *Aedes aegypti* mosquito in Brazil in the 1950s (38-41) following a sustained intervention program that began in the 1930s and 1940s in Rio de Janeiro and other cities (39). Cross-immunity from yellow fever vaccination appears to be very limited (42). Given the young age distribution of the population in 1986 (43), most individuals were not alive during the period when mass yellow fever vaccination or prior dengue epidemics occurred.

We let our time of prediction t_0 be equal to September 1, 1987, corresponding to the end of the initial DENV1 invasion (see panel A of Figure 2). In panel B of Figure 2, we evaluate the number of expected skips expected in Rio de Janeiro, n_c, on the basis of a range of R_0 values from 1.18 to 2.02 from the literature (44, 45). The critical susceptibility threshold for n skips to occur ($s_c(n)$) is calculated using Equation 1 with an annual seasonality, a population growth rate interpolated from the census (see Materials and Methods section), and δ =0.7 (44). The fraction of the population susceptible at the time of the prediction (s_0) is estimated as the difference between the total population N_0 (total population N at (t_0=Sep. 1987)) and the total number of people infected between the start of the invasion and the time of prediction (September 1, 1987). The total number of infected people during the outbreak is computed by summing the ratio between the observed monthly cases and the reporting rate for DENV1 in the city. Literature estimates from serology during the DENV1 invasion in Rio de Janeiro indicate a reporting rate of

220 around 3% (33) which we use and fix for this analysis. For comparison purposes, we also
221 include the number of skips expected under a higher reporting rate of 10%. These curves
222 show that the expected re-emergence could be very sensitive to small variation in R_0 and
223 ρ, two quantities that are difficult to estimate with precision in the absence of serology. In
224 particular, assuming a reporting rate of 3%, a reproductive number of 1.2 with 20%
225 uncertainty can yield large changes in the expected re-emergence time. We highlight the
226 potential sensitivity of the expected number of skips to the reporting rate as well to
227 illustrate the importance of uncertainty in this parameter in cities or epidemics where its
228 value is unknown.

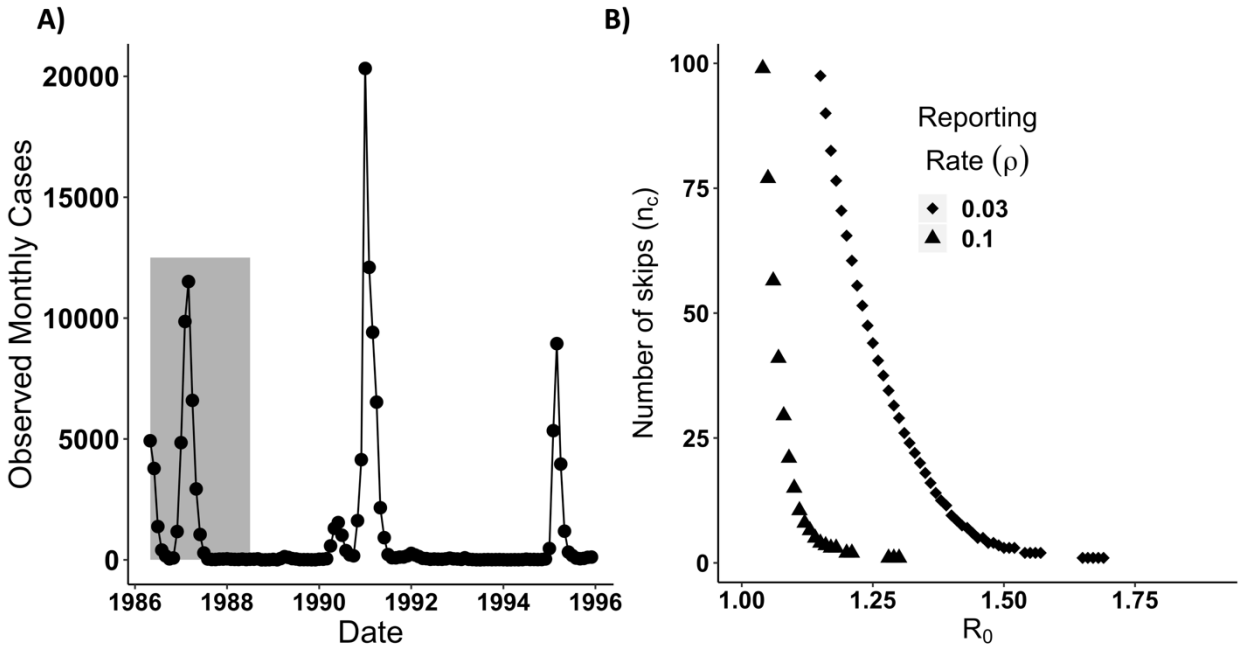

229

230 **Fig 2. (A) Observed dengue case data.** Monthly reported dengue cases in the city of
231 Rio de Janeiro, Brazil from April 1986-1995. The grey shaded region denotes
232 observations that were included in the fitting of the stochastic model from May 1, 1986 to
233 July 1, 1988 inclusive. Serotype DENV1 re-emerged in 1990. DENV2 was first detected
234 in the state of Rio de Janeiro in 1990 but did not become dominant until 1991 (8, 9). Both
235 co-circulated afterwards. We focus on the invasion of DENV1 from 1986-1987 and its
236 initial re-emergence in DENV1 in 1990 using a single serotype transmission model. This
237 allows us to evaluate this transmission model in a region where only one serotype was
238 circulating, where cross-immunity could not easily be invoked to explain the absence or
239 reduction of dengue in a given year. **(B) Deterministic critical number of DENV1 skips**

240 ***n_c* for Rio de Janeiro from September 1988**. Expected number of skips n_c with
241 amplitude of seasonal transmission δ=0.7 and the fraction of the population susceptible
242 after the first DENV1 invasion as of September 1, 1987 (s_0) calculated from the data (A).
243 We use a reporting rate ρ of 3% when calculating s_0 , consistent with serological
244 estimates from the literature (33). For comparison purposes, we also include the expected
245 number of skips n_c assuming a reporting rate of 10%.

246

247

248 **Replenishment of Susceptible Individuals is Insufficient to Explain Re-Emergence**

249 To obtain more precise bounds for the reporting rate and R_0 and to determine if
250 the depletion and replenishment of susceptible individuals could explain the rapid re-
251 emergence of dengue in Rio de Janeiro, we fit a stochastic aggregate SIR model to
252 case data from the DENV1 invasion from 1986-1988. The stochastic SIR model
253 assumes that the underlying deterministic transmission rate varies seasonally as a
254 sinusoidal function with annual mean β_0, seasonal transmission amplitude δ, frequency
255 ω (equal to $2\pi/365$), and phase ϕ. The model takes into account demographic
256 stochasticity, environmental stochasticity in the transmission rate, and measurement
257 error due to under-reporting and variation in reporting of cases (See Materials and
258 Methods and the Supporting Information). Panels A,B, and C of Figure 3 show the
259 likelihood profile of the annual mean transmission rate, β_0, the amplitude of seasonal
260 transmission δ, and the reporting rate ρ, respectively. In particular, our estimate of the
261 reporting rate matches that from serology in the literature (Panel C).

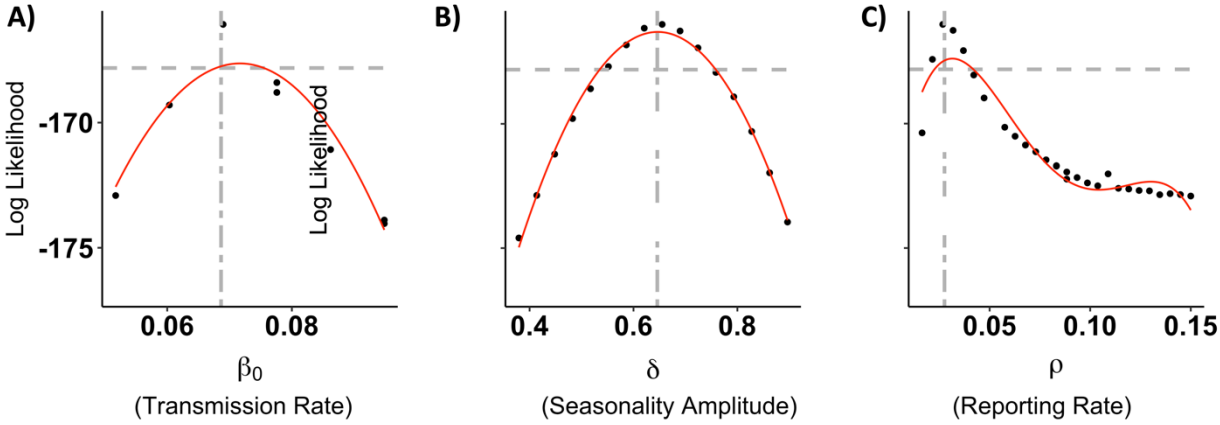

Fig 3. A-C) Selected parameter profiles for the stochastic model. Profiles of the mean annual transmission rate β_0 (A), seasonal transmission amplitude δ (B), and reporting rate ρ (C). The red curve is a polynomial fit to the subset of the profile points shown on the figure. The single dashed grey horizontal line represents the likelihood value 2 log likelihood units below the maximum likelihood estimate. This line provides an estimate of confidence intervals for the given parameter. The grey vertical line denotes the parameter value of the maximum likelihood estimate. The maximum likelihood estimate for the reporting rate in panel C is very close to the literature value obtained from serology (approximately 3 percent). (33).

Overall, the model is able to capture key dynamics of the DENV1 invasion including the two peaks of incidence in 1986 and 1987 and the subsequent reduction of transmission in 1988. This is shown by comparing the trajectories for an ensemble of simulations with the fitted model to the observed values of cases (Fig. 4). Estimated values for the transmission rate indicate a low value for R_0 (Figure 4 Panel C). Both of these conclusions generally hold even if one takes into account uncertainty in parameter estimates by examining all parameter combinations with log likelihoods within 2 log likelihood units of the maximum likelihood estimate (the grey region in Figure 4 Panel C as well as Supplemental Figure S1), although some parameter

combinations (not the maximum likelihood estimate) have substantial process noise (Supplemental Figure S1).

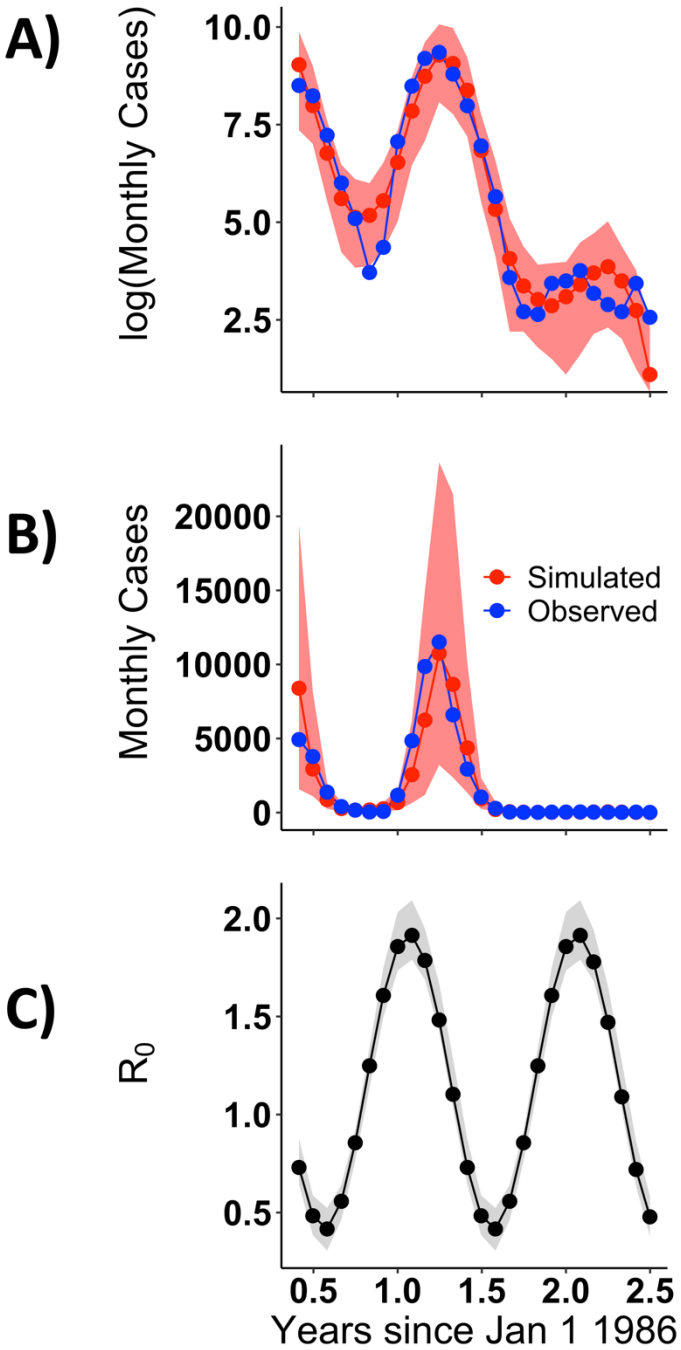

Fig 4. A-B) Comparison of simulated values with the fitted model and observed data on a log (A) and regular (B) scale. Observed monthly cases from April 1986 to June 1988 are shown in blue. Median values from 100 simulations with the maximum likelihood parameter combination are shown in red. The shaded red region denotes the 2.5% and 97.5%th quantile boundaries from those simulations. **C) Estimates for $R_0(t)$.** The black line denotes the trajectory of $R_0(t)$ for the maximum likelihood estimate. The shaded grey region represents the 2.5% and 97.5%th quantile boundaries for trajectories from all parameter combinations within 2 log likelihood units of the maximum likelihood estimate. Each parameter combination has only one seasonal trajectory for $R_0(t)$ since $R_0(t)$ is a deterministic quantity. $R_0(t)$ for all parameter estimates ranges from 1.79-2.09 in the on season to 0.31-0.52 in the off-season.

We now apply the obtained parameter estimates from the fitted model to address the expected re-emergence time on the basis of, first, the analytical expression for the skip calculation (Equation 1), and then the stochastic simulations of the fitted model. The parameter estimates used here are those for the reporting rate ρ, the reproductive number R_0, and the amplitude of seasonal transmission δ from all combinations within 2 log likelihood units of the MLE. The expected number of skips following the DENV1 invasion in 1986-1988 is considerably higher than the observed 2 years. Depending on the parameter combination used, we obtain anywhere from 27 to 100 skips (Panel A of Figure 5). Even the fastest estimated return from the skip analysis (27 years) is much slower than the observed re-emergence time.

Forward simulation of the stochastic model likewise does not predict the rapid re-emergence of DENV1 (Panel B of Figure 5). Under a pulse of 20 infected individuals arriving per day, there was a low probability of re-emergence for parameter combinations with low process noise (Panel B of Figure 5). Only parameter combinations with high amounts of process noise (which have limited predictive value) had a non-zero emergence probability. We consider alternate pulse rates in

316 Supplemental Figure S14. Re-emergence probabilities under forward simulation of the
317 stochastic model thus corroborated the deterministic skip findings. The depletion of
318 susceptible individuals from 1986-1988 and their replenishment via population growth
319 from 1989-1990 under an aggregate SIR model was unable to explain the rapid re-
320 emergence of DENV1 in 1990.

321

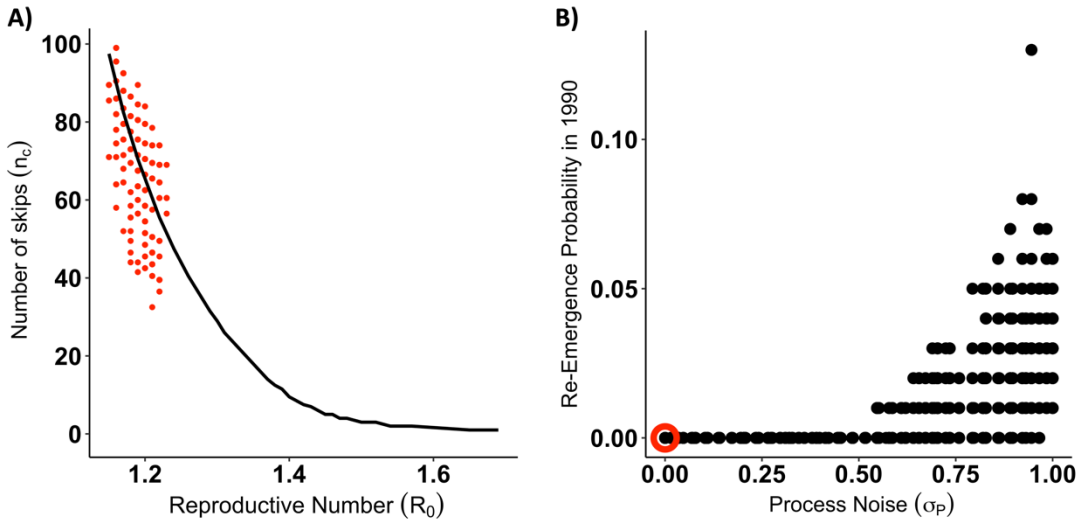

322

323 **Fig 5. A) Expected number of skips (n_c) calculated using parameters obtained**
324 **from the fitted stochastic model.** The open circles show the expected number of
325 skips n_c from Equation 1 using parameters and the fraction of the population susceptible
326 after the initial DENV1 invasion (s_0) estimated from the fitted stochastic model. Each
327 circle corresponds to one parameter combination, and we included here all parameter
328 combinations for the fitted model with a seasonal transmission amplitude (δ) of 0.7 (
329 contacts per person per day) and a likelihood value within two log-likelihood units of the
330 maximum likelihood estimate (MLE). See Figure S15 for expected skips from
331 parameter combinations with different values of δ, and Figure S10 for parameter
332 combinations from the profile of the recovery rate, γ. For comparison purposes, the
333 black line shows the expected number of skips for the deterministic skip calculation from
334 panel B of Figure 2 with the reporting rate ρ fixed at the literature value of 3%. **B)**
335 **Probability of epidemic in 1990 under forward stochastic simulation of fitted**
336 **model.** The fitted stochastic model was simulated forward in time from 1986-1990 with
337 population growth. A pulse of 20 infected individuals were assumed to arrive each day
338 in January 1990. Each parameter combination within 2 log likelihood units of the
339 maximum likelihood estimate was simulated 100 times. The re-emergence probability
340 was calculated by determining the number of simulations in which the susceptible

population decreased in 1990. The plot shows re-emergence probability as a function of the process noise intensity σ_P. Each point represents a single parameter combination. The maximum likelihood estimate parameter combination is circled in red.

Sensitivity Analysis:

To examine the robustness of our findings to adding an incubation period or altering the form of seasonality, we conducted a sensitivity analysis by considering both SIR and SEIR models with spline seasonality. The results are presented and discussed in the Supporting Information and show that our conclusions remain unchanged. (See the Supporting Information including Supplemental Figures S2-S7 and Supplemental Tables ST2 and ST3).

Comparison with Vector Model and literature R_0

The fitted stochastic SIR model uses a cosine function as a simplification to represent the seasonal forcing that would be created by climate variation (temperature (46)) via the changes in infected mosquitos. To evaluate whether this simplification is realistic, we take two approaches. The first one compares the mean seasonal R_0 resulting from our model to values of this reproductive number directly estimated from time series data in the literature for DENV1 and DENV4 in Rio de Janeiro from 2010-2016. There is a close match between these very different ways to estimate R_0, and in particular the shape of the seasonality produced by our model is realistic (Supplemental Figure S18).

The second approach considers a simple temperature-driven vector model. To this end, we initially show that the seasonal variation in temperature in Rio de Janeiro can be approximated via a cosine function (Panel A of Supplemental Figure S19 and use this approximation to drive a transmission rate that includes the vector explicitly.

To obtain an expression for the seasonal transmission rate we consider an explicit mosquito model with compartments for infectious and susceptible mosquitoes in which a number of parameters depend on temperature (*T*) (see Section 4 of the Supporting Information). By assuming fast dynamics of the mosquito (so that levels of infection in the mosquito population quickly equilibrate to the dynamics of infection in the human population), we derive the following expression for the effective transmission rate in the mosquito-human model in terms of the biting rate *a(T)*, probability of human infection given an infectious bite *b(T)*, probability of mosquito infection given biting of an infectious human *pMI(T),* adult mosquito mortality rate μ_M, carrying capacity K of the mosquito population, human population size N, and mosquito demographic function g(T):

$$\beta_{eff} = \frac{a(T)^2 b(T)(pMI(T))}{\mu_M} \frac{K}{N}\left(1 - \frac{\mu_M}{g(T)}\right) \qquad (2)$$

The function g(T) is the product of the eggs laid per female mosquito per gonotrophic cycle, the mosquito egg-to-adult survival probability, and the mosquito egg-adult development rate divided by the adult mosquito mortality rate μ_M. The temperature-dependence of these components was borrowed from the literature (47, 48) (see Supporting Information Section 4 for details).

Under the fast dynamics assumption, this effective transmission rate β_{eff} is an implicit representation of the force of infection inflicted on humans by the vectors of the coupled human-vector model. When re-scaled between 0 and 1, β_{eff} corresponds closely with $\beta_{MLE,}$ the transmission rate from the fitted stochastic SIR cosine model (Panel B of Supplemental Figure S19). This close correspondence indicates that the

389 SIR cosine model is able to capture the shape of the seasonality of DENV1 in Rio de
390 Janeiro.

391

392 ## Discussion

393 We developed two lines of evidence regarding the uncertainty and predictability
394 of the time to re-emergence for diseases with low reproductive numbers, on the basis of
395 a seasonally forced SIR model under the 'well-mixed' assumption at aggregated, city-
396 wide, scales. We showed with an analytical approach that the time to re-emergence
397 (expressed as the number of "skip" years) was highly sensitive to small changes in R_0
398 and the fraction of the population still susceptible s_0 at the time of prediction (e.g. at
399 the end of the initial outbreak). This sensitivity applies to dengue in Rio de Janeiro
400 where re-emergence times can vary on the order of decades based on literature
401 parameters. This uncertainty contrasts with previous applications of this analytical
402 approach to SIR dynamics in childhood diseases such as measles with much higher R_0
403 values where accurate predictions of much shorter skip times have been made (29). We
404 also showed with a stochastic SIR model with seasonal transmission fit to DENV1
405 observed case data for Rio de Janeiro from 1986-1988 that susceptible depletion and
406 replenishment are insufficient to explain dengue re-emergence. The fitted model failed
407 to predict by far the re-emergence of DENV1 in 1990 in terms of either the number of
408 skips expected or the outbreak probability under forward simulation.

409 Transmission parameters like R_0 are generally defined with respect to a particular
410 model. Given that we aggregated cases at the city level and used a short time series,
411 care should be taken in interpreting parameter values. Nevertheless, fitted transmission
412 parameters correspond well with literature values and exhibit well-defined confidence

intervals. Estimates of the reporting rate in particular closely match the 3% value (8) obtained via a serological study conducted during the 1986 invasion (8, 33). Reporting rates during the onset of an epidemic may be much lower in regions that have not recently experienced transmission (33, 49) than in those with re-occurring outbreaks and an established surveillance network. This may explain why serological studies of the 1986 invasion (8, 33) and our results, estimate a lower reporting rate for dengue than studies conducted in later years in Brazil (50). Even though different combinations of the transmission rate and duration of infection can yield the same reproductive number, the parameter estimates that compose R_0 across all models considered in the sensitivity analysis (which take into account those different combinations) are relatively well-defined. These values are also consistent with the effective reproductive number estimated for local dengue epidemics from 2012-2016 (44) and 1996-2014 (45) taking into account differences in serotype circulation and population size during those periods.

More complex model structures are possible and often used for arboviruses that include an explicit representation of the vector. We expect our results to hold as this vector component should largely affect the phase and shape of seasonality in the transmission between human hosts, which we have modeled phenomenologically as a cosine wave. With two typical successive epidemic years from an emergent virus, parameter inference from such short observation period is unlikely to justify a more complex model. Nevertheless, to examine transmission seasonality further, we compared the seasonal R_0 resulting from the fitted model to the seasonal R_0 directly estimated from time series of cases in the literature (44). We also considered the transmission rate experienced by humans in a simple vector-human model forced by the typical seasonality of temperature in Rio de Janeiro. The shape and timing of the

vector-human model's transmission rate was comparable to that of the cosine transmission rate we employed. More complex models that do not assume fast dynamics of infection in the vector relative to epidemic spread would likely exhibit a difference relative to our transmission rate, especially a delayed phase, whose consequences should be examined in future work. We posit that this difference would not influence our results on the predictability and uncertainty of re-emergence, since the values of other parameters (such as the length of infection in humans) can compensate for it.

Factors that could explain the observed rapid re-emergence include inter-annual climate anomalies, antigenic evolution, or micro-scale spatial heterogeneity in transmission intensity and associated susceptible depletion. Larvae washout following flooding coupled with temperature-driven seasonality in transmission could have temporarily halted the invasion in 1988 and delayed the epidemic in 1989. Widespread flooding was reported in February 1988 (51). Large amounts of rainfall washed away mosquito larvae in lab and field studies (52). High rainfall negatively affected dengue transmission in Singapore (53, 54) and India (55). The impact could be compounded in Rio de Janeiro if the high rainfall occurs during the transmission season. If the larvae population has not fully recovered before the start of the off-season, the impact of the rainfall anomaly could extend to the subsequent season.

The large amount of process noise observed in the aggregate model would be consistent with this effect, given that the process noise parameter σ_P represents random variation in the transmission rate due to environmental factors. However, the model's inherent structure limits its ability to take into account flooding events via σ_P, since the magnitude of the process noise does not change between years. Incorporating an inter-

462 annual climate driver could provide more accurate re-emergence predictions. The
463 response to rainfall would be nonlinear: positive at low to moderate levels and negative
464 at higher ones.

465 Intra-serotype antigenic evolution from 1986-1990 could also facilitate faster re-
466 emergence. Many models focus on inter-serotype variation and assume long-lasting
467 homosubtypic immunity (18, 19, 21). However, the antigenic variation within and across
468 dengue serotypes is comparable (56), and antigenic differences between strains of the
469 same serotype influence overall dengue evolution (57). Sequences associated with
470 case data were unavailable, making direct analysis challenging. We cannot rule out the
471 possibility that genetic differences between the circulating strains enabled re-infection. A
472 future SIRS-type model (Susceptible-Infected-Recovered-Susceptible) could
473 incorporate this intra-serotype antigenic evolution.

474 Micro-scale spatial heterogeneity in transmission intensity and the effects of
475 human movement between neighborhoods could also explain the rapid re-emergence.
476 Small-scale differences in socioeconomic status and population density between
477 neighborhoods in a large city can result in different relationships between mosquito and
478 human population sizes, resulting in widespread heterogeneity in R_0 across
479 neighborhoods (58). Previous studies of mosquito trap data in the city have
480 demonstrated that neighborhoods with differing socioeconomic characteristics have
481 different vector population patterns (46). In fact, schoolchildren from neighborhoods
482 with divergent socioeconomic characteristics had varying levels of seroconversion
483 during the 1986 invasion (33). Human movement between neighborhoods may also
484 influence transmission within (59) and between (60) those neighborhoods, potentially
485 resulting in non-uniform depletion of susceptible populations between highly connected

and isolated areas of a city. Whether arising through the effects of spatial heterogeneity in transmission or intra-city movement, non-uniform levels of herd immunity could enable faster re-emergence.

Our findings reveal the uncertainty of re-emergence predictions with the simplest SIR models, those that would be most useful at times of emergent public health threats. Consideration of the above factors in transmission models whose goal is to inform public health over large regions, and to do so soon after, if not during, an emergent outbreak, is clearly a challenge. For example, coarse resolutions are typically used because of the scales at which the observed cases are reported, the scales at which the climate covariates are available, and the difficulties inherent in incorporating microscale variation including connectivity. Our results should motivate further research into the central question of how we can scale microscale heterogeneity to formulate aggregated models that include it implicitly. It should also motivate the related further understanding of how such microscale heterogeneity influences susceptible depletion and replenishment in particular case studies. From such efforts, we should be able to evaluate whether the increasing availability of high-resolution data makes it feasible to parameterize transmission models at higher resolutions, or to inform new model formulations at coarser resolutions.

The inability of susceptible depletion and replenishment in a simple seasonal SIR formulation at a large, city-wide scale, to explain DENV1 re-emergence has potential implications for other arboviruses. Recent long-term Zika forecasts (31) assume that susceptible depletion and replenishment brought an end to the 2015-2017 epidemics and will determine when re-emergence occurs. DENV1 and Zika share the same vector and invaded a completely susceptible population (not accounting for pre-existing cross-

immunity from dengue). If factors absent from the basic model were key drivers of DENV1 inter-annual variability, it would not be unreasonable to infer that similar types of factors could have played a major role in the Zika dynamics observed from 2015-2017. Zika re-emergence could similarly occur much earlier than expected.

With changing temperature patterns due to climate change, cities in Asia, Europe, and the western hemisphere that currently do not have recurrent local transmission may transition in the near future to the kinds of dynamics studied here. Our results suggest that estimates should be interpreted in the context of this sensitivity to small changes in the reporting rate and reproductive number. Factors like variation in reporting rates, micro-scale transmission heterogeneity and inter-annual climate drivers that are often ignored in long-term forecasts may thus become critical in determining re-emergence times. Overall, the large uncertainty in re-mergence times may be unavoidable for these regions. Improved models are needed together with richer data than currently used, to address the question of the relevant spatial scales of susceptible depletion.

Materials and methods

The derivation of the expression for the number of skip years (Equation 1) is included in Section 1 of the Supporting Information. We fitted a stochastic version of the SIR model to observed monthly case counts in Rio de Janeiro from 1986-1988 to estimate parameters needed to apply this expression, and also to separately predict in parallel the time to re-emergence via numerical simulation Expected re-emergence times were then compared for the two approaches.

Data Description

We used monthly dengue case estimates in the city of Rio de Janeiro, Brazil from 1986-1990. Cases were reported to the local public health surveillance system (9, 10). The case counts did not contain serotype information, but prior studies indicated that the dengue serotype DENV1 invaded the city of Rio de Janeiro in 1986 (10) and was the dominant serotype in circulation in the state of Rio de Janeiro from 1986-1990 (8) prior to the arrival of DENV2 in 1990. DENV2 did not become dominant until 1991 (9).

Basic Model Formulation

Because dengue infection confers full immunity to the same serotype, we considered an SIR (Susceptible-Infected-Recovered) model. The deterministic model for the number of individuals in the Susceptible *(S)*, Infected (*I*), or Recovered (*R)* class is given by the following system of ordinary differential equations:

$$\frac{dS}{dt} = rN - \lambda(t)S - \mu_H S \quad (3)$$

$$\frac{dI}{dt} = \lambda(t)S - \gamma I - \mu_H I \quad (4)$$

$$\frac{dR}{dt} = \gamma I - \mu_H R \quad (4)$$

$$\lambda(t) = \beta(t)\left(\frac{I}{N}\right) \quad (5)$$

552

553 $$\beta(t) = \beta_0(1 + \delta sin(\omega t + \phi)) \quad (6)$$

554 Deaths occur at rate (μ_H) given by the inverse of the life expectancy of Brazil in
555 2012 (74.49 years(35)). All individuals are born susceptible. The term *r* represents
556 population growth. The human population growth rate was estimated from census
557 resident population estimates in 1991 (36) and 2000 (37) assuming exponential growth.
558 This rate was used to interpolate the estimated population in 1986 (See Supporting
559 Information Section 2.1.1 for details).

560 The per capita rate at which susceptible individuals become infected was given
561 by the force of infection $\lambda(t)$ (Equation 5). Individuals recovered at per-capita rate γ
562 whose inverse is the duration of infection. Estimates of the duration of infection in
563 dengue vary. One analysis estimated that symptoms of dengue infection last 2-7 days
564 following an incubation period of 4-10 days (61, 62). For our analysis, we fixed the
565 recovery rate γ to be 1/17, assuming an exponentially distributed duration of infection
566 with mean of 17 days encapsulating the maximum extent of the combined incubation
567 and symptomatic period in humans. We take into account the possibility that duration of
568 infection could vary by profiling over the duration of infection in the sensitivity analysis.
569 The short duration of the available time series meant that fitting a formal vector model
570 could prove difficult and could require additional assumptions in terms of which
571 parameters could be fitted or fixed from existing formulations in the literature. We
572 therefore used an SIR framework in which the infected stage served as a proxy for the
573 exposed and infected human and vector compartments in a vector model of dengue
574 transmission. A duration of infection was thus chosen to also take into account the

575 external incubation period in the mosquito, which can range from 5-33 days at 25°C to
576 2-15 days at 30°C (63). We profiled over the duration of infection in the sensitivity
577 analysis to verify that this parameterization is reasonable.

578 This transmission rate $\beta(t)$ was represented as a cosine function with mean β_0,
579 (units of contacts per person per day) and seasonal oscillations of amplitude δ (same
580 units as β_0) and frequency ω, which was assumed to be annual ($\omega = 2\pi/365$) days^{-1}. The
581 annual mean R_0 was thus given by:

582
$$R_0 = \frac{\beta_0}{\gamma + \mu} \quad (8)$$

583 The observed dengue data in Rio de Janeiro consisted of monthly case counts.
584 Serological studies of the DENV1 invasion in Rio de Janeiro also indicated substantial
585 under-reporting (8, 33). Let C represent the true number of monthly cases that would be
586 obtained by summing the number of individuals entering the infected class (I) over the
587 course of a month. For the purposes of the skip analysis, we assume that a fixed
588 fraction ρ of the true cases C are observed, where ρ is the reporting rate.

589 The stochastic model is an approximation of the deterministic one used for the
590 skip analysis. For simplicity and given the short time interval, we assumed that there
591 was no population growth over the two and half years of the DENV1 invasion ($r = \mu_H$)
592 and that births and deaths occurred at rate μ_H = (1/(74.9*365)), which is equal to the
593 inverse of the average life expectancy in Brazil from the 2010 census (35). However,
594 population growth is taken into account when simulating forward in time from the fitted
595 stochastic model. We also assumed that there were no recovered individuals at the start

of the epidemic, so all other individuals in the population not initially infected were susceptible. We considered time in units of days and used a time step Δt of 1 day.

The stochastic model is a discrete-time model with fixed time step Δt and a discrete state space (i.e. the number of people in each compartment *S*, *I, R*, and *C*, at any point in time must be integers). The number of individuals who moved from one compartment to another over the course of each day was calculated via Euler simulation from the deterministic equations (See Supporting Information). Demographic stochasticity was then incorporated into the Euler approximations to obtain integer state variable values after each time step. We specifically assumed that the number of individuals making each state transition was drawn from a binomial distribution with exponentially decaying probability (See Supporting Information). Environmental noise (variation in the transmission rate $\beta(t)$ due to random environmental variation) was captured via multiplicative gamma white noise in the transmission rate as described by (64, 65). On time step size Δ t, we multiplied the transmission rate by $\Delta\Gamma / \Delta$ t, where $\Delta\Gamma / \Delta$ t was drawn from a Gamma distribution with mean 1 and variance σ_P^2 / Δ t.

The measurement model assumed that the observed number of monthly dengue cases ($Y(t)$) at time t were drawn from a negative binomial distribution with mean equal to the true number of monthly cases C multiplied by a reporting rate ρ, with dispersion parameter σ_M. More details of the measurement model can be found in Section 2.4 of the Supporting Information.

Fitting the stochastic model

We fitted the transmission parameters (β_0 and δ), reporting rate (ρ), process noise parameter (σ_P), measurement noise parameter (σ_M), and the number of infected

individuals at the start of the outbreak in May 1986 (I_0). While the first cases of DENV1 were reported in April 1986, we started the model fitting in May 1986 to avoid complications from changes in the reporting rate as the surveillance system was established during the start of the DENV1 invasion. We used in an interpolated initial population size of 528,1842 for Rio de Janeiro in May 1986.The model was fit using the mif2 method in the R-package pomp. The model fitting method is described further in the Supporting Information and in (66).

Calculating expected skips using parameter estimates from stochastic model

Following the completion of the Monte Carlo Profiles, final parameter combinations from all profiles were pooled together to obtain both a maximum likelihood estimate (MLE) parameter combination as well as all parameter combinations that were within 2 log likelihood units of the maximum likelihood estimate. The table of MLE parameter values is shown in Supplemental Table ST1. The reporting rate (ρ), β_0, and δ value of each parameter combination within 2 log likelihood units of the maximum likelihood estimate were applied to a finer gridded version of the deterministic skip calculation described earlier. A distribution for the number of skips expected in Rio de Janeiro following the DENV1 invasion from 1986-1988 was obtained.

Stochastic Simulation

We then simulated re-emergence probabilities under the stochastic model. Each parameter combination within 2 log likelihood units of the MLE estimate from the stochastic fit was simulated again without any immigration from 1986 until 1990 but with population growth. During January 1990, “sparks” of infectious individuals were assumed to have arrived in the city at some fixed rate. We explored rates from 5 to 100 infected individuals per day. This process was repeated 100 times, and the probability

of an epidemic occurring in 1990 was calculated. An epidemic occurrence in this situation was defined as a net decrease in the susceptible population over the course of the year (after taking into account population growth), to best match the definition of an epidemic used in the skip analysis.

Sensitivity Analysis

We assessed how parameter estimates of R_0 and ρ may depend on the model formulation by fitting several more complex SIR-type models to the same data using the fitting procedure described in the Methods section: an SIR Spline Model and SEIR Spline Model. As an additional sensitivity analysis, we profiled over the recovery rate for the SIR Cosine Model (Supplemental Figure S9). For details, see the Supporting Information.

Comparison with Vector Model and literature R_0

For a full description of the explicit coupled human-mosquito model with compartments for infectious and susceptible mosquitoes and comparison of transmission rates between this model and the simpler seasonally forced SIR , see the Supporting Information.

References

1. Bhatt S, Gething PW, Brady OJ, Messina JP, Farlow AW, Moyes CL, et al. The global distribution and burden of dengue. Nature. 2013;496(7446):504.
2. Baud D, Gubler DJ, Schaub B, Lanteri MC, Musso D. An update on Zika virus infection. The Lancet. 2017;390(10107):2099-109.
3. Petersen LR, Jamieson DJ, Powers AM, Honein MA. Zika Virus. New England Journal of Medicine. 2016;374(16):1552-63.
4. Nasci RS. Movement of Chikungunya Virus into the Western Hemisphere. Emerging Infectious Diseases. 2014;20(8):1394-5.

5. Nogueira RM, Eppinghaus AL. Dengue virus type 4 arrives in the state of Rio de Janeiro: a challenge for epidemiological surveillance and control. Memórias do Instituto Oswaldo Cruz. 2011;106:255-6.
6. Zanluca C, de Melo VCA, Mosimann ALP, dos Santos GIV, dos Santos CND, Luz K. First report of autochthonous transmission of Zika virus in Brazil. Memórias do Instituto Oswaldo Cruz. 2015;110(4):569-72.
7. Nunes MRT, Faria NR, de Vasconcelos JM, Golding N, Kraemer MUG, de Oliveira LF, et al. Emergence and potential for spread of Chikungunya virus in Brazil. BMC Medicine. 2015;13(1):102.
8. Nogueira RMR, Miagostovich MP, Schatzmayr HG, Santos FBd, Araújo ESMd, Filippis AMBd, et al. Dengue in the State of Rio de Janeiro, Brazil, 1986-1998. Memórias do Instituto Oswaldo Cruz. 1999;94:297-304.
9. Nogueira RMR, Miagostovich MP, Lampe E, Souza RW, Zagne SMO, Schatzmayr HG. Dengue Epidemic in the State of Rio de Janeiro, Brazil, 1990-1: Co-Circulation of Dengue 1 and Dengue 2 Serotypes. Epidemiol Infect. 1993;111(1):163-70.
10. Miagostovich MP, Nogueira RM, Cavalcanti S, Marzochi KB, Schatzmayr HG. Dengue epidemic in the state of Rio de Janeiro, Brazil: virological and epidemiological aspects. Revista do Instituto de Medicina Tropical de São Paulo. 1993;35(2):149-54.
11. O'Reilly KM, Lowe R, Edmunds WJ, Mayaud P, Kucharski A, Eggo RM, et al. Projecting the end of the Zika virus epidemic in Latin America: a modelling analysis. BMC medicine. 2018;16(1):180-.
12. Struchiner CJ, Rocklöv J, Wilder-Smith A, Massad E. Increasing Dengue Incidence in Singapore over the Past 40 Years: Population Growth, Climate and Mobility. PLOS ONE. 2015;10(8):e0136286.
13. Stewart-Ibarra AM, Lowe R. Climate and non-climate drivers of dengue epidemics in southern coastal ecuador. Am J Trop Med Hyg. 2013;88(5):971-81.
14. Vincenti-Gonzalez MF, Tami A, Lizarazo EF, Grillet ME. ENSO-driven climate variability promotes periodic major outbreaks of dengue in Venezuela. Scientific reports. 2018;8(1):5727-.
15. Hii YL, Rocklöv J, Ng N, Tang CS, Pang FY, Sauerborn R. Climate variability and increase in intensity and magnitude of dengue incidence in Singapore. Global Health Action. 2009;2(1):2036.
16. Harris M, Caldwell JM, Mordecai EA. Climate drives spatial variation in Zika epidemics in Latin America. bioRxiv. 2019:454454.
17. Cazelles B, Chavez M, McMichael AJ, Hales S. Nonstationary Influence of El Niño on the Synchronous Dengue Epidemics in Thailand. PLOS Medicine. 2005;2(4):e106.
18. Recker M, Blyuss Konstantin B, Simmons Cameron P, Hien Tran T, Wills B, Farrar J, et al. Immunological serotype interactions and their effect on the epidemiological pattern of dengue. Proceedings of the Royal Society B: Biological Sciences. 2009;276(1667):2541-8.
19. Reich NG, Shrestha S, King AA, Rohani P, Lessler J, Kalayanarooj S, et al. Interactions between serotypes of dengue highlight epidemiological impact of cross-immunity. Journal of The Royal Society Interface. 2013;10(86).
20. Cummings DAT, Schwartz IB, Billings L, Shaw LB, Burke DS. Dynamic effects of antibody-dependent enhancement on the fitness of viruses. Proceedings of the National Academy of Sciences of the United States of America. 2005;102(42):15259.
21. Ferguson N, Anderson R, Gupta S. The effect of antibody-dependent enhancement on the transmission dynamics and persistence of multiple-strain pathogens. Proceedings of the National Academy of Sciences of the United States of America. 1999;96(2):790-4.

718 22. Bjørnstad ON, Finkenstädt BF, Grenfell BT. Dynamics of measles epidemics: estimating
719 scaling of transmission rates using a time series SIR model. Ecological Monographs.
720 2002;72(2):169-84.
721 23. Earn DJD, Rohani P, Bolker BM, Grenfell BT. A Simple Model for Complex Dynamical
722 Transitions in Epidemics. Science. 2000;287(5453):667-70.
723 24. Finkenstädt B, Grenfell B. Empirical determinants of measles metapopulation dynamics
724 in England and Wales. Proc Biol Sci. 1998;265(1392):211-20.
725 25. Graham M, Winter AK, Ferrari M, Grenfell B, Moss WJ, Azman AS, et al. Measles and
726 the canonical path to elimination. Science. 2019;364(6440):584-7.
727 26. Grenfell BT, Bjørnstad ON, Finkenstädt BF. DYNAMICS OF MEASLES EPIDEMICS:
728 SCALING NOISE, DETERMINISM, AND PREDICTABILITY WITH THE TSIR MODEL.
729 Ecological Monographs. 2002;72(2):185-202.
730 27. Domenech de Cellès M, Magpantay FMG, King AA, Rohani P. The impact of past
731 vaccination coverage and immunity on pertussis resurgence. Science Translational Medicine.
732 2018;10(434):eaaj1748.
733 28. Lavine JS, King AA, Bjørnstad ON. Natural immune boosting in pertussis dynamics and
734 the potential for long-term vaccine failure. Proceedings of the National Academy of Sciences.
735 2011;108(17):7259-64.
736 29. Stone L, Olinky R, Huppert A. Seasonal dynamics of recurrent epidemics. Nature.
737 2007;446(7135):533.
738 30. Lowe R, Bailey TC, Stephenson DB, Jupp TE, Graham RJ, Barcellos C, et al. The
739 development of an early warning system for climate-sensitive disease risk with a focus on
740 dengue epidemics in Southeast Brazil. Statistics in medicine. 2012;32(5):864-83.
741 31. Ferguson NM, Cucunubá ZM, Dorigatti I, Nedjati-Gilani GL, Donnelly CA, Basáñez M-
742 G, et al. Countering the Zika epidemic in Latin America. Science. 2016;353(6297):353-4.
743 32. Imai N, Dorigatti I, Cauchemez S, Ferguson NM. Estimating Dengue Transmission
744 Intensity from Case-Notification Data from Multiple Countries. PLOS Neglected Tropical
745 Diseases. 2016;10(7):e0004833.
746 33. Figueiredo LTM, Cavalcante SMB, Simoes MC. Dengue serologic survey of
747 schoolchildren in Rio de Janeiro, Brazil, in 1986 and 1987. 1990.
748 34. Olinky R, Huppert A, Stone L. Seasonal dynamics and thresholds governing recurrent
749 epidemics. Journal of Mathematical Biology. 2008;56(6):827-39.
750 35. (IBGE) BIoGaS. Brazil Demographic Census 2010. . Rio de Janeiro, Brazil: Brazilian
751 Institute of Geography and Statistics (IBGE). 2012.
752 36. (IBGE) BIoGaS. "Censo Demographico- 1991-Rio de Janeiro". 1991;"Censo
753 demográfico : 1991 : resultados do universo relativos as características da população e dos
754 domicílios"(Table 1.4: "População residente, por grupos de idade, segundo ti lolesorregiàes, as
755 Microrregiões, os Municípios,os Distritos e o sexo"):32-41.
756 37. (IBGE) BIoGaS. Censo Demográfico. 2000(População residente, sexo e situação do
757 domicílio; Total column).
758 38. Dick OB, San Martín JL, Montoya RH, del Diego J, Zambrano B, Dayan GH. The
759 history of dengue outbreaks in the Americas. The American journal of tropical medicine and
760 hygiene. 2012;87(4):584-93.
761 39. Severo OP. Eradication of the Aedes aegypti mosquito from the Americas. 1955.
762 40. Löwy I. Leaking Containers: Success and Failure in Controlling the Mosquito Aedes
763 aegypti in Brazil. Am J Public Health. 2017;107(4):517-24.
764 41. PAHO. The feasibility of erradicating Aedes aegypti in the Americas. Pan Am J Public
765 Health. 1997;1.

42. Souza NCSe, Félix AC, de Paula AV, Levi JE, Pannuti CS, Romano CM. Evaluation of serological cross-reactivity between yellow fever and other flaviviruses. International Journal of Infectious Diseases. 2019;81:4-5.
43. de Carvalho JAM. Demographic dynamics in Brazil: recent trends and perspectives. Brazilian journal of population studies. 1997;1(1):5-23.
44. Codeço CT, Villela DA, Coelho FC. Estimating the effective reproduction number of dengue considering temperature-dependent generation intervals. Epidemics. 2018;25:101-11.
45. Coelho FC, Carvalho LMd. Estimating the Attack Ratio of Dengue Epidemics under Time-varying Force of Infection using Aggregated Notification Data. Scientific Reports. 2015;5:18455.
46. Honório NA, Codeço CT, Alves FC, Magalhães MAFM, Lourenço-de-Oliveira R. Temporal Distribution of Aedes aegypti in Different Districts of Rio De Janeiro, Brazil, Measured by Two Types of Traps. Journal of Medical Entomology. 2009;46(5):1001-14.
47. Mordecai EA, Cohen JM, Evans MV, Gudapati P, Johnson LR, Lippi CA, et al. Detecting the impact of temperature on transmission of Zika, dengue, and chikungunya using mechanistic models. PLOS Neglected Tropical Diseases. 2017;11(4):e0005568.
48. Otero M, Schweigmann N, Solari HG. A Stochastic Spatial Dynamical Model for Aedes Aegypti. Bulletin of Mathematical Biology. 2008;70(5):1297.
49. Musa SS, Zhao S, Chan H-S, Jin Z, He D. A mathematical model to study the 2014–2015 large-scale dengue epidemics in Kaohsiung and Tainan cities in Taiwan, China. Mathematical biosciences and engineering. 2019.
50. Imai N, Dorigatti I, Cauchemez S, Ferguson NM. Estimating dengue transmission intensity from sero-prevalence surveys in multiple countries. PLoS neglected tropical diseases. 2015;9(4):e0003719-e.
51. Ap. 127 Die in Floods and Mud Slides in Brazil. New York Times. 1988 02/08/ 1988 Feb 08.
52. Fouque F, Carinci R, Gaborit P, Issaly J, Bicout DJ, Sabatier P. Aedes aegypti survival and dengue transmission patterns in French Guiana. Journal of Vector Ecology. 2006;31(2):390-400.
53. Benedum CM, Seidahmed OME, Eltahir EAB, Markuzon N. Statistical modeling of the effect of rainfall flushing on dengue transmission in Singapore. PLOS Neglected Tropical Diseases. 2018;12(12):e0006935.
54. Seidahmed OME, Eltahir EAB. A Sequence of Flushing and Drying of Breeding Habitats of Aedes aegypti (L.) Prior to the Low Dengue Season in Singapore. PLOS Neglected Tropical Diseases. 2016;10(7):e0004842.
55. Kakarla SG, Caminade C, Mutheneni SR, Morse AP, Upadhyayula SM, Kadiri MR, et al. Lag effect of climatic variables on dengue burden in India. Epidemiol Infect. 2019;147:e170.
56. Katzelnick LC, Fonville JM, Gromowski GD, Arriaga JB, Green A, James SL, et al. Dengue viruses cluster antigenically but not as discrete serotypes. Science. 2015;349(6254):1338.
57. Bell S, Katzelnick L, Bedford T. Dengue antigenic relationships predict evolutionary dynamics. bioRxiv. 2019:432054.
58. Romeo-Aznar V, Paul R, Telle O, Pascual M. Mosquito-borne transmission in urban landscapes: the missing link between vector abundance and human density. Proceedings of the Royal Society B: Biological Sciences. 2018;285(1884):20180826.
59. Stoddard ST, Forshey BM, Morrison AC, Paz-Soldan VA, Vazquez-Prokopec GM, Astete H, et al. House-to-house human movement drives dengue virus transmission. Proceedings of the National Academy of Sciences. 2013;110(3):994-9.

60. Guzzetta G, Marques-Toledo CA, Rosà R, Teixeira M, Merler S. Quantifying the spatial spread of dengue in a non-endemic Brazilian metropolis via transmission chain reconstruction. Nature Communications. 2018;9(1):2837.
61. Organization WH. Dengue and severe dengue. Fact sheet Updated April 2017. 2017.
62. Organization WH. Dengue and severe dengue. World Health Organization. Regional Office for the Eastern Mediterranean; 2014.
63. Chan M, Johansson MA. The Incubation Periods of Dengue Viruses. PLOS ONE. 2012;7(11):e50972.
64. Bretó C, Ionides EL. Compound markov counting processes and their applications to modeling infinitesimally over-dispersed systems. Stochastic Processes and their Applications. 2011;121(11):2571-91.
65. He D, Ionides EL, King AA. Plug-and-play inference for disease dynamics: measles in large and small populations as a case study. Journal of the Royal Society Interface. 2009;7(43):271-83.
66. Ionides EL, Nguyen D, Atchadé Y, Stoev S, King AA. Inference for dynamic and latent variable models via iterated, perturbed Bayes maps. Proceedings of the National Academy of Sciences. 2015;112(3):719-24.